Journal of Alloys and Compounds 509 (2011) 4252–4259

Contents lists available at ScienceDirect

Journal of Alloys and Compounds

journal homepage: www.elsevier.com/locate/jallcom

Hydrogen absorption and desorption characteristics of high coercivity NdDyFeCoNbCuB sintered magnet. I. Low temperature hydrogen decrepitation treatments

J.J. Luo[a,b], P. de Rango[b,c], D. Fruchart[b,c,*], J.N. Mei[a,c], L. Zhou[a]

[a] State Key Laboratory of Solidification Processing, NPU, Xi'an 710072, PR China
[b] Groupe IICE, Département MCMF, Institut Néel, CNRS, 38042 Grenoble Cedex 9, France
[c] CRETA, CNRS, 38042 Grenoble Cedex 9, France

ARTICLE INFO

Article history:
Received 31 March 2010
Received in revised form 15 October 2010
Accepted 21 October 2010
Available online 30 October 2010

Keywords:
Hydrogen decrepitation
Hydrogen desorption
NdDyFeCoNbCuB sintered magnets

ABSTRACT

Hydrogen absorption/adsorption properties of high coercivity NdDyFeCoNbCuB sintered magnets were determined. Hydrogenation kinetics were analyzed using both differential scanning calorimetry (DSC) and X-ray diffraction (XRD). Hydrogenation of the Nd-rich intergranular phase results in a rather broad and large peak at ~100 ± 50 °C, then the tetragonal main phase (Φ phase) reacts readily close to 195 °C. The disproportionation process of the whole magnet initiates at $T \sim 500$ °C, then accelerates in the vicinity of 600 °C and finally ends at $T \sim 780$ °C. Furthermore, the first hydrogenation reaction, which is associated with the hydrogen diffusion in the bulk via the intergranular Nd-rich phase, was seen to proceed quite differently depending on the heating rate, or the applied plateau temperature. While hydrogen absorption at 50 °C is rather slow, it results in higher hydrogen uptake than at 150 °C, though there it happens much faster. Three modes of hydrogenation of sintered magnets are discussed in terms of practical operability. Using the optimized hydrogen decrepitation/desorption annealing route leads to a demonstration that the anisotropic NdDyFeCoNbCuB powders obtained by the HD/D technique have recovered most of the magnetic performance initially displayed in the bulk magnets.

© 2010 Elsevier B.V. All rights reserved.

1. Introduction

Since the first demonstration of their particularly hard magnetic properties in 1984 [1,2], $Nd_2Fe_{14}B$ based magnets have been rapidly optimized and used for many applications. At present, the need for high coercivity H_c and energy product $(B{\cdot}H)_{max}$ requires the addition of specific rare earth elements such as Dy. However, these types of elements are much more expensive than Nd because of their lower abundance. Furthermore, there are new pressing questions issued from the increasing resource depletion for all RE elements, and more particularly Nd. Besides, another economic question emerges with the increasing waste of NdFeB magnet products and also with increasing enforcement of environmental legislations. Since there exists a strong demand for anisotropic NdFeB powder for the production of bonded magnets, it is attractive to transform wastes of sintered NdFeB magnets into coercive and anisotropic powders by exploiting the HDDR process [3–7].

$Nd_2Fe_{14}B$ was reported to absorb significant amounts of hydrogen at room temperature and under moderate pressure [7] and the effects of hydrogenation on the structural, chemical, physical and mechanical properties have been established from further successive works [6,8–12]. The relatively large expansion in lattice parameters upon hydrogenation induces a decrepitation process, leading to the easy production of very fine magnetic particles [3,5,12,13]. The so-called "hydrogen decrepitation (HD)" process has been used to prepare anisotropic powder from magnetically textured material, e.g. bulk NdFeB sintered magnets [5,14–17]. On the other hand, die-upset MQ3 materials [18], hot-rolled NdFeB ingots [19], hot-forged NdFeCuB ingots [15] and sintered NdDyFeNbAlB bulk magnets were synthesized using the so called "powder technology processes", for use in hard disk drives [20]. However, it is of common knowledge that crushing, milling and other mechanical and energy consuming treatments, which reduce a bulk material from rough to fine powders, may lead to a reduction in remanence and coercivity. Moreover, the milling process should also preserve the nominal chemical composition, to avoid further oxidization, which is not so easy when processing μm sized highly reacting particles. Conversely, high temperature hydrogen atmosphere exposure leads to more or less the complete disproportionation of the NdFeB phase. Based on such a reaction,

* Corresponding author at: Groupe IICE, Département MCMF, Institut Néel, CNRS, 38042 Grenoble Cedex 9, France. Tel.: +33 4 76 88 11 43; fax: +33 4 76 88 10 38.
E-mail address: daniel.fruchart@grenoble.cnrs.fr (D. Fruchart).

0925-8388/$ – see front matter © 2010 Elsevier B.V. All rights reserved.
doi:10.1016/j.jallcom.2010.10.093

Table 1
Comparison of the best magnetic performances of precursor bulk magnets and the corresponding bonded HD50 and HD150 submitted to hydrogen and high temperature treatments.

Parameters	Precursor magnet	Powders HD at 50 °C	Powders HD at 150 °C	Recovery rate HD50
Remanence, B_r	11.1 kG 1.11 T	9.7 kG 9.7 T	6.1–9.7 kG 6.1–9.7 T	87%
Intrinsic coercivity, H_{cj}	30.9 kOe 2460 kA/m	12.6 kOe 1300 kA/m	7.5–9.75 kOe597–776 kA/m	41%
Maximum energy product, $B{\cdot}H_{max}$	29.4 MGOe234 kJ/m^3	16.9 MGOe134.5 kJ/m^3	16.7 MGOe 133 kJ/m^3	68%

Takeshita and Nakayama [21] opened the way to deliver very high coercivity levels in NdFeB powders after a second treatment that consists to outgas hydrogen and to recombine the solid elements at rather high temperature. Harris and co-workers [22] have rationalized the process, thus called HDDR (Hydrogen-Disproportionation-Dehydrogenation-Recombination), his group and later many other ones having designed different variants of the HDDR process. Though high values of coercivity has been achieved, the values of remanence of HDDR-processed material is modest compared to those achieved in sintered NdFeB magnets. In addition, sub-micron sized HDDR-treated powders are rather sensitive to corrosion.

Earlier it was shown that a typical ternary NdFeB ingot (i.e. a piece of magnet) absorbs or reacts with hydrogen via three distinct steps, and later it desorbs the hydrogen at three successive stages [21–23]. These are hydrogenation of the main Φ phase, hydrogenation of the R-rich interstitial phase and formation of RH_x hydrides upon disproportionation. Hydrogenation processes of NdFeB materials can be quantified by two parameters [22,23]: (1) the amount of reacted hydrogen and (2) the rate of feeding with hydrogen under H_2 pressure close to normal. By a proper control of these parameters, given states or full hydrogenation of the Nd-rich phase and/or the Φ phase can be obtained. It is worth to note that amplification of the specific surface resulting from HD of the sample can accelerate hydrogenation kinetics by about 5-orders of magnitude [24].

Bulk NdDyFeCoNbCuB magnets were developed having improved thermal stability [1,25–27] for high temperature applications (e.g. the electrical motor of hybrid cars). The need for recycling and re-use is all the more important since some of the additional elements used in these magnets (Dy, Co) are the most expensive elements in these powerful NdFeB based magnets.

In the present paper, we report on hydrogenation absorption and desorption processes applied to a selected NdDyFeCoNbCuB composition. The at.% formula of that magnet material is $Nd_{11.9}Dy_2Tb_{0.5}Fe_{72.4}Co_5Nb_{1.5}Cu_{0.3}Ga_{0.4}B_6$. We discuss the anisotropic and coercive characteristics of powders that can be prepared by application of the Hydrogen Decrepitation/Dehydrogenation process (HD/D). More particularly we focus here on the first step that consists in the HD procedure as operated at low or medium temperature. In a further report we will present optimized results from variants of the second step, that is the D-dehydrogenation procedure developed at high temperature. It is obvious that such global treatments can be applied advantageously to freshly produced magnet scraps as well as to recycle old magnets.

2. Experimental

Two types of measurements – titration and DSC analysis – have been applied in order to quantify the hydrogen absorption and desorption characteristics of NdDyFeCoNbCuB sintered magnets [28]. The magnetic alloys manufactured at NIN (Northwestern Institute for Non-ferrous Materials) at Xi'an, China, are characterized by high coercivity and medium level remanence as displayed in Table 1. SEM, EDX and X-ray diffraction analysis have shown that the tetragonal phase (Φ phase) present as the main magnet component has the overall formula $(Nd,Dy)_2(Fe,Co,Nb,Cu)_{14}B$ (here after shortly written as $R_2M_{14}B$).

Differential scanning calorimeter (DSC) measurements were performed using a Netzsch DSC404S working under a flow of mixed gases ($Ar+H_2$) at a rate of 100 ml/min. The H_2 gas flow rate was 10 ml/min and the working temperature ranged from room temperature to 1000 °C at a heating or cooling rate of 30 K/min.

Hydrogenation kinetic measurements were performed using a Hydrogen Titration System GenIII (Base B). The mass of sample used for this experiment was about 655 mg. The amount of hydrogen gained by the sample during the absorption reaction was estimated from the hydrogen pressure changes. Two hydrogen absorption processes were performed at 50 °C and 150 °C respectively under a hydrogen pressure of 70 kPa. For both samples, the hydrogen desorption process was performed at 300 °C under primary vacuum.

Besides, the samples were analyzed systematically after each step of the treatment firstly by SEM using a Jeol JSM5600LV equipped with EDX, and secondly by X-ray diffraction in Bragg-Brentano mode using a Philips PW 3830 power supply.

To prepare anisotropic powders, pieces of bulk magnet were decrepitated first and then the powders were submitted to hydrogen desorption under secondary vacuum first at 400 °C for at least 2 h and then at temperature ranging from 820 to 880 °C for 1 h. Following this, the powders were annealed at ~500 °C for 1 h. The magnetic performance of these powders was measured on dense samples in a form of bonded-type magnets which were prepared by mixing an epoxy resin with the annealed powers crushed lightly by hand. The composites were compacted and placed under a magnetic field of 5 T to orientate the fine powders during gluing, before being magnetically analyzed with an extraction magnetometer.

3. Results

3.1. DSC measurements

Three large exothermic peaks can be seen on the DSC trace displayed in Fig. 1. A first exothermic peak occurred in the temperature range of 40–185 °C. It can be seen in Fig. 1 that this corresponds to the hydrogenation of the R-rich phase as checked by X-ray diffraction. The pattern plotted in Fig. 2 demonstrates that the Nd-rich phase was almost fully hydrogenated but the tetragonal phase (Φ phase) remained mostly unreacted with hydrogen.

A second exothermic peak was recorded in the temperature range of 185–220 °C, corresponding to the simultaneous hydrogenation of the R-rich phase and the $R_2M_{14}B$ phase, as shown from the diffraction pattern of Fig. 2. At such temperatures, hydrogen molecules can split on the surface and atoms can diffuse rapidly to the core of the $R_2M_{14}B$ particles. This is the typical temperature range where the Φ phase absorbs hydrogen [7].

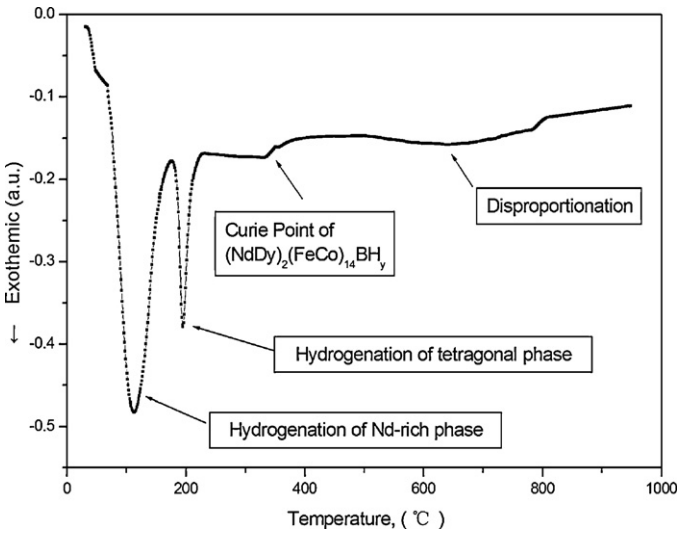

Fig. 1. Hydrogenation DSC trace of a NdDyFeCoNbCuB sintered magnet.

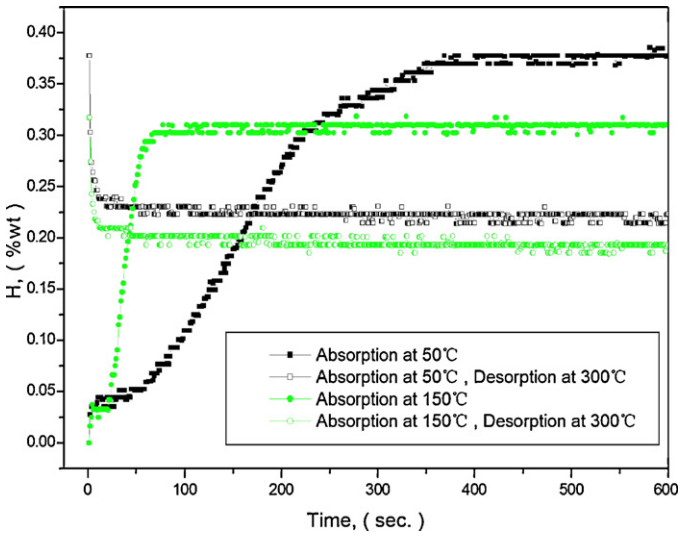

Fig. 2. XRD patterns recorded at different stages of the DSC scan, where the most significant peaks have been pointed out: a, bulk magnet (squares for $Nd_2Fe_{14}B$); b, after the 1st DSC peak (squares for $Nd_2Fe_{14}B$, dot for NdH_x); c, after the 2nd DSC peak (upward-triangles for $Nd_2Fe_{14}BH_{1.04}$, dot for NdH_x); d, after ending the DSC measurement at high temperature (downward-triangles for α-Fe).

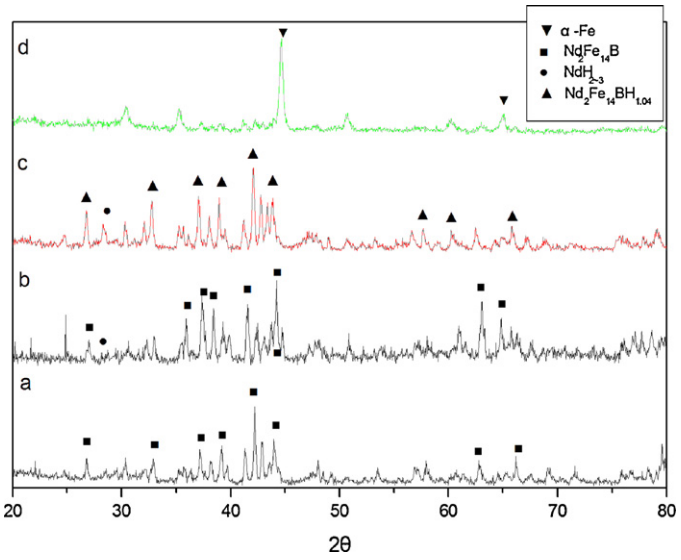

Fig. 3. Hydrogen absorption kinetics traces recorded at 50 and 150 °C under 70 kPa H_2 gas pressure, and the corresponding desorption traces recorded at 300 °C under primary vacuum.

Then a small transition occurs around 360 °C as shown in Fig. 1. This peak corresponds well to the Curie temperature of $R_2M_{14}BH_x$, measured in by thermomagnetic analysis [28].

A third exothermic peak that corresponds to the decomposition reaction (disproportionation) of $R_2M_{14}BH_x$, presents a broad and flat profile in the wide range of 450–800 °C, as displayed in Fig. 1. This exothermal peak looks rather different to that evidenced by Book and Harris [29], who recorded a sharp and narrow peak at disproportionation during DTA measurements under 1 bar H_2 pressure. In our case, the flat signal can be correlated to the limited hydrogen partial pressure applied during the measurement leading to a softer process according to the as monitored penetration and diffusion process in the Φ phase grains.

3.2. Hydrogenation kinetics analysis

3.2.1. Absorption

As shown in Fig. 3, relatively slow hydrogen absorption occurs after a short incubation period when the temperature of the sample was initially stabilized at 50 °C. During the process, the exothermal reaction leads the sample to a moderate increase of temperature of $\Delta T \sim 12.5$ °C. Completing the experiment, the overall hydrogen absorption reaches the saturation value of 0.38 ± 0.02 wt% (realized after ~360 min), thus corresponding to the overall formula $(Nd,Dy)_{15}(Fe,Co,Nb,Cu)_{79}B_6H_x$ with $x = 25.5 \pm 0.2$.

Conversely and as reported also in Fig. 3, fast hydrogen absorption occurs at 150 °C after a shorter incubation period leading to a hydrogenation saturation value of 0.31 ± 0.02 wt% realized after ~80 s. It corresponds to the overall formula $(Nd,Dy)_{15}(Fe,Co,Nb,Cu)_{79}B_6H_x$ with $x = 21 \pm 0.2$. Correspondingly, the exothermal rise of temperature of the sample is $\Delta T \sim 46.5$ °C.

The temperature rise of the sample during hydrogen absorption at 150 °C is ~4-times higher than that recorded at 50 °C, meaning that the hydrogenation reaction is much more vigorous when activated at 150 °C than at 50 °C. Unexpectedly, the overall hydrogen uptake is more marked when processed at 50 °C than at 150 °C. In fact this can be related to the rate of heat extraction from the present sample. Since the temperature of 150 °C is quite close to the equilibrium temperature at normal H_2 pressure leading to the reaction $R_2Fe_{14}B \leftrightarrow R_2Fe_{14}B{\cdot}H_{xmax}$ ($x_{max} = 5.5$ [7]), a less efficient extraction of heat developed in the $R_2M_{14}B$ sample due to exothermal reaction according to the rate of supplying H_2 gas leads to a reduction of the hydrogen uptake when occurring in the range of the transition temperature. Such a limiting phenomenon has been observed to occur when hydrogenating different types of metal hydrides, e.g. when forming MgH_2 [30].

These results agree fairly well with those obtained using XRD analysis of the hydrogenated samples. As shown in Fig. 4b and c, the hydride of tetragonal Φ phase has a nominal formula of $R_2M_{14}BH_{1.85}$ when the sample was hydrogenated at 50 °C while the resulting formula is $R_2M_{14}BH_{1.05}$ when it was hydrogenated at 150 °C.

Simultaneously, the R-rich phase always exhibits the same hydrogen content for both processing temperatures, agreeing well with the nominal formula $RH_{2.4}$ as deduced from Fig. 4a and d.

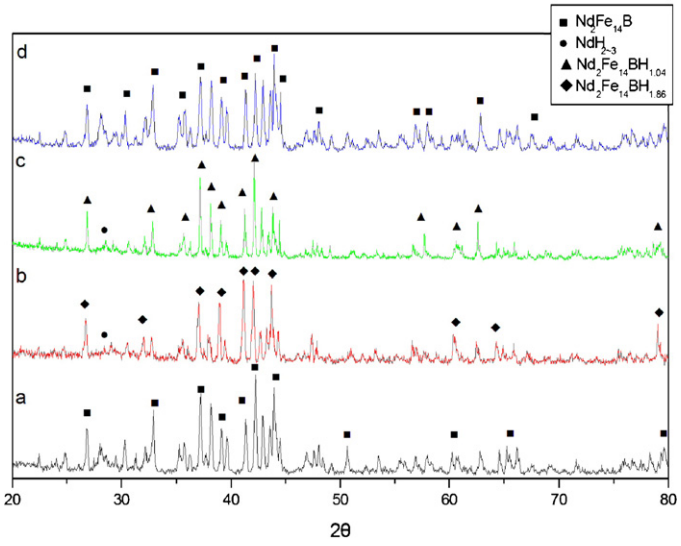

Fig. 4. XRD patterns after hydrogen absorption at 70 kPa H_2 gas pressure in NdDyFeCoNbCuB under various temperature conditions, where the most significant peaks have been pointed out: a, absorption at 50 °C (squares for $Nd_2Fe_{14}B$), desorption at 300 °C; b, absorption at 50 °C (lozenges for $Nd_2Fe_{14}BH_{1.86}$, dot for NdH_x); c, absorption at 150 °C (upward triangles for $Nd_2Fe_{14}BH_{1.04}$, dot for NdH_x); d, absorption at 150 °C, desorption at 300 °C (squares for $Nd_2Fe_{14}B$).

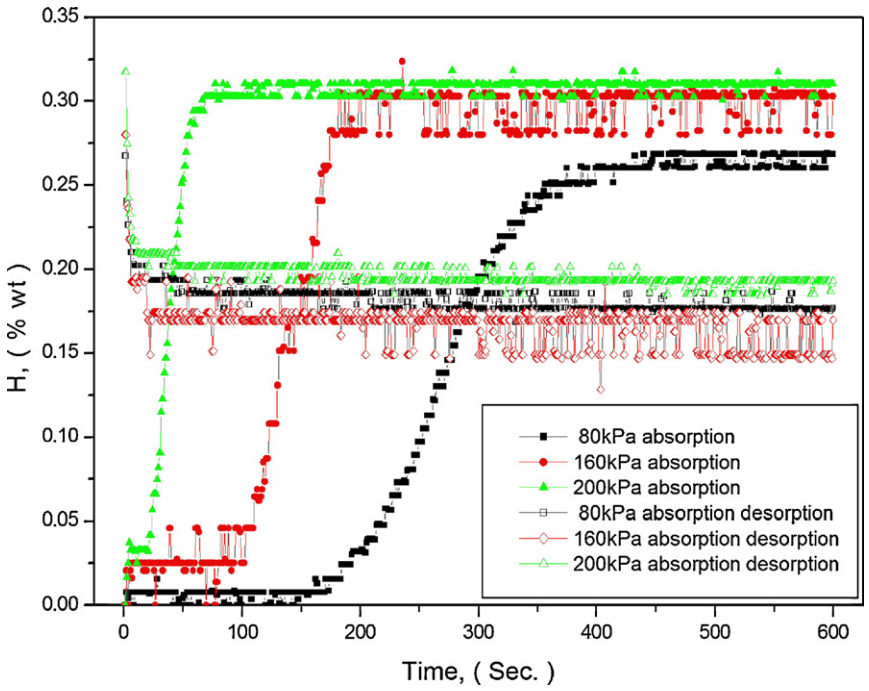

Fig. 5. Hydrogen absorption kinetics traces recorded at 150 °C and the corresponding desorption traces recorded at 300 °C under primary vacuum.

Thereby, the larger amount of absorbed hydrogen in the sample when realized in moderate conditions contributes to the hydrogenation of the tetragonal phase. Also the samples appear homogeneously H-treated; for each case Fig. 4 indicates the presence of unique hydrogenated phases, thus hydrogen is quite homogeneously distributed in the main Φ and the minor R-rich phases.

Rescaling versus time and versus amplitude the two absorption traces displayed in Fig. 3 allow the consideration of a unique absorption process whatever the temperature. If both traces reveal an early incubation process that can be attributed to a similar nucleation-propagation mechanism, the trace recorded at 50 °C evolves in a more complicated manner than that recorded at 150 °C. A two-step absorption phenomenon takes a sigmoid type progression for ~2/3 of elapsed time and ~3/4 of the absorbed hydrogen, and an almost linear absorption progression for the remaining time and ~1/6 of the total amount of absorbed hydrogen. This behavior should be correlated to the evidence of 2 absorption peaks as observed in DSC analysis shown in Fig. 1.

A series of samples have been prepared applying two successive HD processes, with intermediate desorption at 300 °C only. In this case, the intergranular Nd-rich phase remains hydrogenated and does not react again at the second hydrogenation. Then the absorption reaction was undertaken under different H_2 gas pressures at 150 °C as shown in Fig. 5. The reaction times (s) and amount of absorbed hydrogen (wt%) corresponding to the second reaction cycle are represented in Fig. 6. Two typical times are considered, the first corresponding to the incubation time of the reaction, the second to the faster absorption period. It is clear that both these characteristics decrease with the applied pressure, but if the first one decreases in a quadratic manner, being almost equal to zero for $P > 200$ kPa H_2 pressure, the second process decreases in an exponential manner with applied pressure. This should be interpreted in terms of two thermally activated processes. In this case, the heat of formation of the Nd-rich phase hydride does not occur. Consequently, the incubation time is much longer, as compared to that of Fig. 3 at 70 kPa. However, diffusion of hydrogen to form the $R_2M_{14}B$ hydride should behave as a van't Hoff type equilibrium. Besides, the total amount of absorbed hydrogen decreases smoothly and linearly upon increasing the applied pressure, but it appears fairly proportional to the time needed to reach saturation, which obviously decreases when H_2 pressure is increased.

3.2.2. Desorption

As shown in Fig. 3, hydrogen desorption occurs very rapidly at 300 °C under primary vacuum (10^{-2} atm) without any incubation period, no matter whether the hydrogen was charged at

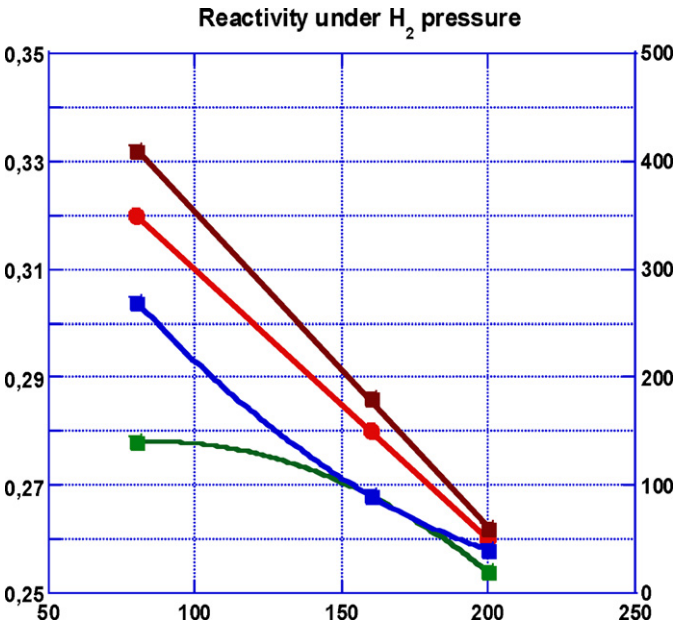

Fig. 6. Analysis of the hydrogen uptake and reaction kinetics at 150 °C and under 80, 160 and 200 kPa H_2 gas pressure. Red dots: amount of absorbed hydrogen (wt%); blue squares: activation-nucleation process (s); green squares: absorption–diffusion rate (s) of hydrogen in the NdDyFeCoNbCuB material; black squares: time to reach hydrogen saturated uptake (sum of the two previous data).

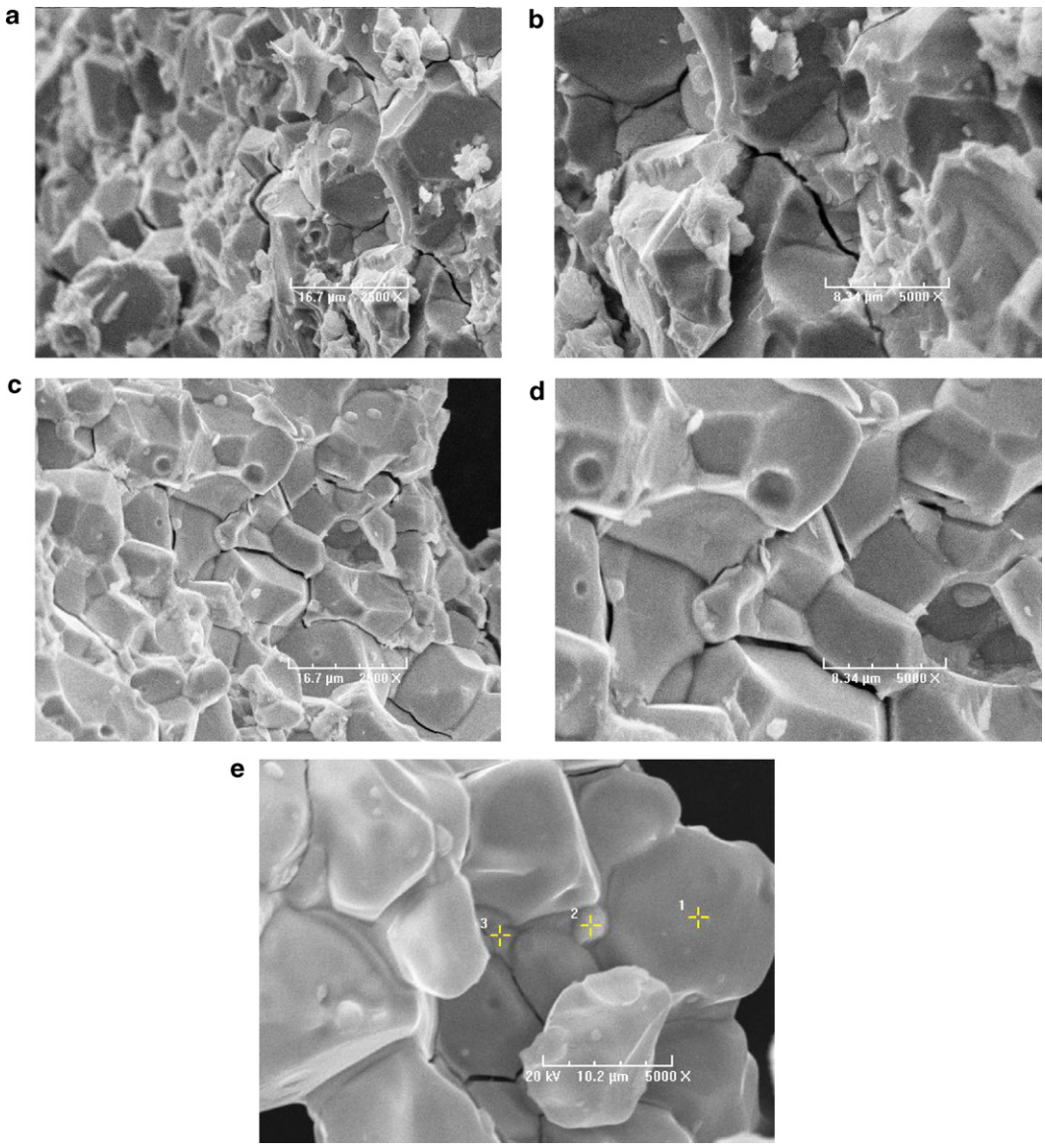

Fig. 7. (a) SEM pictures for the decrepitated powder HDT050. (a) ×2500 (marker = 16.7 μm); (b) ×5000 (marker = 8.34 μm). (b) SEM pictures for the decrepitated powder HDT150 (a) ×2500 (marker = 16.7 μm); (b) ×5000 (marker = 8.34 μm). (c) SEM picture of a decrepitated powder desorbed at 800 °C: ×5000 (marker = 8.34 μm).

50 °C or at 150 °C. The sample that was hydrogen charged at 50 °C releases a relative hydrogen mass of ~0.154 wt%, while the second one which was charged at 150 °C desorbs a relative mass of 0.119 wt%. This confirms that the sample which has absorbed more (less) hydrogen at 50 °C (150 °C) desorbs more (less) hydrogen at 300 °C. It is worth to note that the remaining hydrogen is approximately 0.21 ± 0.02 wt%. Accordingly, the hydrogen desorbed from $(NdDy)_{15}(FeCoNbCu)_{79}B_6H_x$ at 300 °C should correspond to the main amount of hydrogen absorbed by the $R_2M_{14}BH_x$ phase. This is corroborated also by XRD data as displayed in Fig. 4a and d, where no trace of the $Nd_2Fe_{14}BH_x$ system can be noticed, conversely to that of the hydrogenated R-rich phase, which practically desorbs at much higher temperatures than 300 °C.

3.2.3. Magnetic performances

The magnetic performances of a magnet are defined by the coercive field H_c, the remanent magnetization B_r and the maximum energy product $(B{\cdot}H)_{max}$ that characterizes the squareness of the hysteresis cycle. As said above, achievement of optimized magnet properties of the hydrogen treated NdFeB type magnets needs the application of further high temperature treatments firstly to fully desorb hydrogen and secondly to optimize the (magnetic) microstructure. Thus, both types of HD powders (at 50 and 150 °C) were submitted to hydrogen desorption under secondary vacuum first at 400 °C for least 2 h and then at 840 °C for 1 h and finally they were annealed at 510 °C for 1 h.

It is obvious that to some extent such high temperature treatments tend to erase more or less peculiar material features induced during a given decrepitation cycle, since at the highest applied temperatures the intergranular Nd-rich phase is melted. From Fig. 7a and b, it looks rather difficult to characterize distinctly the morphology of both types of decrepitated powders produced by the HD procedure applied at 50 °C (HD50) and 150 °C (HD150). However, it is clear that after a complete dehydrogenation and subsequent heat treatments the surface and the sharp aspect of the grains have been smoothed as shown in Fig. 7c.

Measured magnetic performances of HD/D treated anisotropic materials are summarized in Table 1 and a hysteresis loop is traced in Fig. 8. Interestingly, the remanence B_r was rather well recovered, while the coercivity H_c of bulk magnets can also be recovered but to a more limited extent. Several reasons can be considered for the reduced coercivity of HD/D magnets, being direct causes (e.g.

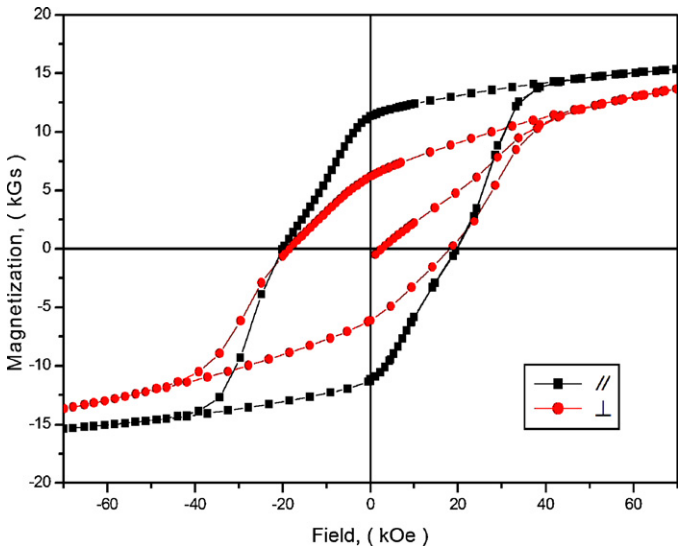

Fig. 8. Hysteretic loop for the HD/D anisotropic powders.

size and shape of particles, homogeneity of the microstructure) or indirect ones (effect of dispersion, coating with resin, etc.) [15,18]. The maximum energy product $(B{\cdot}H)_{max}$ was rather well restored (~70%) but neither fully recovered up to the initial value, as evidenced by a limited squareness of the de-magnetization curve as shown in Fig. 8. From the many treatments and experiments proceeded on the HD50 and HD150, it clearly appears that processing at 150 °C leads to much lower recovery or coercivity than when processing at 50 °C, or even at room temperature (not shown here).

The microstructure of these powders was observed by SEM as shown in Fig. 7. It reveals that intergranular fracture is the main occurring phenomenon. However, HD50 samples exhibit more evidence of intra-granular fracture than HD150 samples. Since intra-granular fracture leads to more fresh surfaces embedded in Nd-rich phase, this could be one reason for the rather higher values of coercivity achieved in the HD50 samples. This means that the first step of the HD process has a marked impact on the performances of the final bonded magnets. Besides, it is well known that the coercive level depends mainly on the high temperature procedure, since no significant coercivity is expected from just hydrogenated samples. In fact, the better coercivity recovery with the HD50 samples, means that the optimized final heat treatments are applied to powders of finer grain size, owing to the greater number of intra-granular cracks developed during HD. Finally, Table 2 displays even more optimized data, effectively achieved after applying several variants of the second step treatment (dehydrogenation-annealing). So, magnetic performances of HD processed bonded magnets can be restored to better levels, provided the final heat treatments of the powders are also optimized, thus definitively favoring the HD50 treated materials. These arguments will be developed in a forthcoming paper especially devoted to variants of the dehydrogenation process, that could be again improved in the future, e.g. to $(B{\cdot}H)_{max}$ better than 80% of that of the initial bulk precursors.

Table 2
HD50 powders as treated at different set of temperatures as above for dehydrogenation and annealing.

Parameters	Optimized HD50 powders	Recovery rate reference to precursor
Remanence, B_r	11.3 kG 1.13 T	102
Intrinsic coercivity, H_{cj}	20.0 kOe 1592 kA/m	65
Maximum energy product, BH_{max}	23.4 MGOe 186.3 kJ/m^3	80

4. Discussion

From hydrogenation kinetics and DSC measurements, it was demonstrated that NdDyFeCoNbCuB sintered magnet samples absorb and desorb relatively more hydrogen at 50 °C than at 150 °C. This was attributed to the absorption rate of the main Φ phase of global formula $R_2M_{14}B$, with respectively 1.85 and 1.05 H atom/unit formula. The kinetics of reaction of samples absorbing hydrogen are unexpectedly different when processed at 50 and 150 °C, respectively. Moreover, a pressure sensitive phenomenon was identified with the latter type treatment only.

As thermal treatments usually accelerate hydrogen uptake of metals and alloys, moderate heating (up to 100 to 200 °C) is a unique activation procedure used to efficiently form metal hydrides. The present HD results as well as the final extrinsic magnet performances achieved in two series of bonded magnets made with the HD50 and HD150 powders need to be analyzed in terms of structural transformation and deformation.

Coming back to the hydrogen site filling scheme developed earlier to explain the structure of the $Nd_2Fe_{14}BH_x$ ($0 < x < 5.5$) [7], one should consider the amount of hydrogen effectively inserted in the present boride at 50 and 150 °C, respectively. Hydrogen insertion in $Nd_2Fe_{14}B$ type compounds involves four types of R-rich tetrahedral sites in the crystal cell of the Φ phase, among which two are mostly active for hydrogen absorption. According to nomenclature of the $P4_2/nmm$ space group of the $R_2Fe_{14}B$ type structure, one has to consider first the (4e) sites ($r_i > 0.5$ Å, 3R-1Fe) and the (8j) site ($r_i \sim 0.45$ Å, 2R-2Fe). The two other active tetrahedral sites, ($16k_1$) and ($16k_2$) ($r_i \leq 0.4$ Å), have been reported to be less attractive in terms of chemical environment and insertion radius [9,12]. Making reference to Westlakes's rules [31], it is worth to recall that the maximum hydrogen uptake (5.5 H/f.u.) corresponds to a statistical half occupation of all these four active sites, the local occupation numbers being 0.5H, 2H, 1H and 1H for the (4e), (8j), ($16k_1$) and ($16k_2$), respectively. Here, one has also to consider that Dy, with a smaller atomic radius than Nd, and both Co and Cu with lower affinity for hydrogen than Fe, are probably limiting factors leading to a restricted H-uptake of less than 5.5 H/f.u., moreover under moderate pressure conditions [32].

For the HD50 and HD150 samples, the respective Φ-hydride phase formula was established to be $R_2M_{14}BH_{1.85}$ and $R_2M_{14}BH_{1.05}$, respectively. For these hydrogen quantities, one will consider that hydrogen saturates the (8j) sites and almost fills the (16k) sites simultaneously for $R_2M_{14}BH_{1.85}$ (HD50) and again saturates the (8j) sites but fills with a lower amount of hydrogen only the (16k) sites for $R_2M_{14}BH_{1.05}$ (HD150) [9]. This can be understood in terms of overall bonding energy of hydrogen atoms which decreases upon increasing temperature, thus at 150 °C, hydrogen atoms are less bonding in the (8j) site, as the result of equilibrium pressure/temperature conditions. At desorption, the relative filling scheme of the concerned tetrahedral sites will operate in the reverse way. This tendency was asserted from the DSC experiments as reported in Fig. 2, in which after reaching the second hydrogenation peak, the as-received Φ phase hydride was found (mass and XRD measurements) to have also a composition close to $R_2M_{14}BH_{\sim 1.0}$.

If however it was reported that under 100 kPa H_2 gas pressure, the ternary Φ phase only absorbs hydrogen at around 200 °C [29], here we find that hydrogen reacts with the Nd-rich and Φ phase simultaneously both at 50 and 150 °C under 70 kPa H_2 pressure as shown in Figs. 4 and 5, in agreement with earlier experiments [32].

Correspondingly, Turek et al. [24] have reported that H_2 gas can react simultaneously with the Nd-rich and the Φ phase by appropriate selection of hydrogenation parameters. As for many cases of metal hydrogenation, the freshness and surface state make that hydrogenation can occur along different routes when treated under moderate conditions. Indeed, the global formula and the overall microstructure of materials as well as other extrinsic characteristics need to be considered.

Three types of reactions have happened during the hydrogen absorption process, as shown in Eqs. (1)–(3):

$$\text{Nd-rich} + (x/2)H_2 \leftrightarrow \text{Nd-rich}\,H_x \quad \text{(intergranular reaction)} \qquad (1)$$

$$Nd_2Fe_{14}B + (y/2)H_2 \leftrightarrow Nd_2Fe_{14}BH_y \quad (\Phi\text{-phase reaction}) \qquad (2)$$

$$Nd_2Fe_{14}B + zH_2 \leftrightarrow NdH_z + \alpha\text{-Fe} + \text{“FeB}'' \quad \text{(HDDRreaction)} \qquad (3)$$

Firstly H_2 reacts with the Nd-rich phase (Eq. (1)), secondly hydrogen reacts directly (H_2 – Eq. (2)) or indirectly (Eq. (1) – H) with the Φ-phase depending on the temperature. Thirdly, hydrogen atoms bond directly with Nd, thus leading to the disproportionation of both metal phases, a phenomenon here practically excluded at the operating temperatures and pressure (Eq. (3)).

It is generally accepted that during the first absorption process, a marked volume change affects the hydrogenated Nd-rich phase and causes intergranular cracks between the grains of the Φ phase. In parallel, a lot of free surfaces of Nd-rich phase and Φ phase develop continuously, easing the advance of hydrogen [12]. However, providing little (HD50) or much more heat, (HD150), the second type of uptake can be either activated (H from Nd-rich H_x to Φ) or inhibited owing to thermodynamic equilibrium conditions (H_2 to Φ). Thus, depending on the final relative H-uptake, intragranular cracks can affect the main Φ-phase grains. It is worth to recall that a total hydrogen saturation of the Φ phase to the hydride formula $Nd_2Fe_{14}BH_{5.5}$ leads to a nearly isotropic volume cell expansion ($\Delta a/a \sim 1.1\%$, $\Delta c/c \sim 1.0\%$) [9,10], the expansion proceeds in several successive steps, concerning the *a* cell parameter first then the *c* cell parameter and finally *a* again as illustrated in [32]. If the (4e) sites can be considered of negligible impact due to the little amount of H-uptake and a more symmetrical situation of those sites, filling the (8j) sites leads to a fully anisotropic expansion scheme favoring the (a,b) basal plane dilatation in the early stage of hydrogenation [9]. Accordingly it has been well established that the increase of Curie temperature of the $Nd_2Fe_{14}BH_x$ versus *x*, is much more accentuated at the early stage of hydrogenation, owing to the bond length expansion of anomalously short Fe–Fe distances, effectively lying parallel to the basal plane.

So, hydrogen uptake in $R_2M_{14}B$ up to ~2 H at./f.u. might lead to the development of anisotropic stresses in the hydrogenated Φ phase $R_2M_{14}BH_x$ grains, which should result in more specifically oriented intragranular cracks at decrepitation. Such a phenomenon cannot occur for less hydrogen uptake (e.g. $0 < x < 1.0$), moreover isotropic cell expansion occurs at larger H-uptakes.

Finally, a finer control of the hydrogenation process (HD) of solid materials having been processed first as bulk magnets would likely deliver anisotropic particles having higher values of remanence. This is the main consideration to fulfill in order to establish an optimized low temperature HD/D treatment, enabling the development of high performance powders for the bonded magnet applications.

5. Conclusion

Hydrogen absorption and desorption characteristics in NdDyFeCoNbCuB sintered magnets was studied by DSC and hydrogenation kinetic measurements. Coercive and anisotropic powders were prepared by the HD/D process (Hydrogen Decrepitation/Dehydrogenation) and results on both procedures and performances are presented in this paper.

(1) DSC measurements show that bulk magnets absorb hydrogen at different temperatures, thus reacting readily close to 120 °C, then a second but weaker hydrogen absorption is identified close to 200 °C, finally the disproportionation of the crystallized phases happens within a broad temperature range from around 450 °C to 800 °C.
(2) Hydrogenation kinetic measurements show that hydrogen absorption happens more rapidly at 150 °C than at 50 °C, while less hydrogen is absorbed at 150 °C than at 50 °C.
(3) Anisotropic NdDyFeCoNbCuB powders obtained by the HD/D technique can recover the magnetic characteristics of the starting bulk magnet, provided the hydrogenation procedure (HD) is optimized. It is anticipated that some level of intragranular fracture occurs, in addition to the main intergranular decrepitation.
(4) The magnetic performance of HD/D powders can close to those of the starting materials if both the HD and D steps are operated in well defined conditions (profiles of heating/cooling down, temperatures of reactions, H_2 gas pressures, etc.). This will be described in a forthcoming paper.

Acknowledgements

The authors thank the French Embassy in Beijing for providing a PhD grant to one of us (J.-J.L.) as a contribution to the collaborative research program of the LIA-LAS2M linking NIN – NPU Xi'an, China and CNRS, Grenoble, France. Thanks are due to N.M. Dempsey, J.L. Soubeyroux (Institut Néel) and S. Rivoirard (CRETA) for helpful discussions.

References

[1] J.J. Croat, J.F. Herbst, R.W. Lee, F.E. Pinkerton, J. Appl. Phys. 55 (1984) 2078.
[2] M. Sagawa, S. Fujimura, N. Togawa, H. Yamamoto, Y. Matsuura, J. Appl. Phys. 55 (1984) 2083.
[3] P. Dalmas de Réotier, D. Fruchart, R. Fruchart, R. Guillen, P. L'Héritier, P. Vulliet, P. Wolfers, A. Yaouanc, J. Phys. 46 (1985) 323.
[4] H.H. Stadelmaier, N.C. Liu, Mater. Lett. 4 (1986) 304.
[5] D. Fruchart, S. Miraglia, R. Perrier de la Bâthie, R. Fruchart, P. Mollard, Patent EP 90 06-206, 1991.
[6] D. Fruchart, M. Bacmann, P. de Rango, O. Isnard, S. Liesert, S. Miraglia, S. Obbade, J.L. Soubeyroux, E. Tomey, P. Wolfers, J. Alloys Compd. 253–254 (1997) 121.
[7] D. Fruchart, P. Wolfers, P. Vulliet, A. Yaouanc, R. Fruchart, P. L'Héritier, in: I.V. Mitchell (Ed.), Nd–Fe Permanent Magnets—Their Present and Future Applications, CEC, Brussels, 1984.
[8] P. Dalmas de Réotier, D. Fruchart, L. Pontonnier, F. Vaillant, P. Wolfers, A. Yaouanc, J.M.D. Coey, R. Fruchart, P. L'Héritier, J. Less-Common Met. 129 (1987) 133.
[9] D. Fruchart, S. Miraglia, S. Obbade, P. Ezekwenna, Ph. L'Heritier, J. Magn. Magn. Mater. 83 (1990) 291.
[10] P. Wolfers, M. Bacmann, D. Fruchart, J. Alloys Compd. 317–318 (2001) 39.
[11] V.A. Yartys, O. Gutfleisch, V.V. Panasyuk, I.R. Harris, J. Alloys Compd. 253–254 (1997) 128.
[12] D. Fruchart, S. Miraglia, P. de Rango, P. Wolfers, J. Alloys Compd. 383 (2004) 17.
[13] I.R. Harris, C. Noble, T. Bailey, J. Less-Common Met. 106 (1985) L1.
[14] S. Liesert, PhD Thesis, Université J. Fourier, Grenoble, France, 1998.
[15] S. Rivoirard, J.G. Noudem, P. de Rango, D. Fruchart, S. Liesert, J.L. Soubeyroux, Proceedings of the 16th Internatioanl Workshop on Rare-earth Magnets and Their Applications, vol. 347–354, Kyoto, Japan, 2000.
[16] S. Namkung, A.S. Kim, D.H. Kim, T.S. Jang, D.H. Lee, H.W. Kwon, D.H. Hwang, HPMA'04, Proceedings of the 18th International Workshop on High Performance Magnets and their Applications, Annecy, France, 2004.
[17] H.W. Kwon, D.H. Hwang, I.C. Jeong, A.S. Kim, D.H. Kim, S. Namkung, T.S. Jang, D.H. Lee, HPMA'04, Proceedings of the 18th International Workshop on High Performance Magnets and their Applications, Annecy, France, 2004.
[18] M. Doser, R.W. Ribitsch, J.J. Croat, V. Panchanathan, J. Appl. Phys. 69 (1991) 5835.
[19] D. Hinz, A. Handstein, I.R. Harris, IEEE Trans. Magn. 30 (1994) 601.
[20] C.C. Huang, S.B. John, S.S. Bor, Energ. Convers. 14 (4) (1999) 1259.
[21] T. Takeshita, R. Nakayama, 10th International Workshop on Rare Earth Magnets and Their Applications, vol. 551–557, Kyoto, Japan, 1989.

[22] M. Zakotnik, I.R. Harris, A.J. Williams, J. Alloys Compd. 450 (1–2) (2008) 525.
[23] A.J. Williams, P.J. McGuiness, I.R. Harris, J. Less-Common Met. 171 (1991) 149.
[24] K. Turek, P. Liszkowaki, H. Figiel, J. Alloys Compd. 309 (2000) 239.
[25] P. Liszkowski, K. Turek, H. Figiel, J. Alloys Compd. 307 (2000) 297.
[26] S. Hirosawa, S. Mino, H. Tomizawa, J. Appl. Phys. 69 (1991) 5844.
[27] L.H. Lewis, K. Gallagher, V. Panchanathan, J. Appl. Phys. 85 (1999) 5926.
[28] C.D. Fuerst, E.G. Brewer, Appl. Phys. Lett. 56 (1990) 2252.
[29] D. Book, I.R. Harris, J. Alloys Compd. 221 (1995) 187.
[30] J. Charbonnier, P. de Rango, D. Fruchart, S. Miraglia, L. Pontonnier, S. Rivoirard, N. Skryabina, P. Vuillet, J. Alloys Compd. 383 (2004) 205.
[31] D.G. Westlake, J. Less-Common Met. 103 (1984) 203.
[32] S. Liesert, PhD, University J. Fourier, Grenoble, France, 1998.